

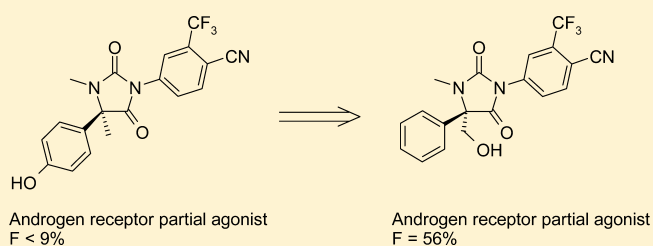
Identification of a 4-(Hydroxymethyl)diarylhydantoin as a Selective Androgen Receptor Modulator

François Nique, Séverine Hebbe, Nicolas Triballeau, Christophe Peixoto, Jean-Michel Lefrançois, Hélène Jary, Luke Alvey, Murielle Manioc, Christopher Housseman, Hugo Klaassen,[†] Kris Van Beeck, Denis Guédin,[‡] Florence Namour, Dominique Minet, Ellen Van der Aar, Jean Feyen, Stephen Fletcher, Roland Blanqué, Catherine Robin-Jagerschmidt, and Pierre Deprez*

GALAPAGOS, Parc Biocitech, 102 Avenue Gaston Roussel, 93230 Romainville, France

S Supporting Information

ABSTRACT: Structural modification performed on a 4-methyl-4-(4-hydroxyphenyl)hydantoin series is described which resulted in the development of a new series of 4-(hydroxymethyl)diarylhydantoin analogues as potent, partial agonists of the human androgen receptor. This led to the identification of (*S*)-(-)-4-(4-(hydroxymethyl)-3-methyl-2,5-dioxo-4-phenylimidazolidin-1-yl)-2-(trifluoromethyl)benzonitrile ((*S*)-(-)-**18a**, GLPG0492) evaluated *in vivo* in a classical model of orchidectomized rat. In this model, (-)-**18a** exhibited anabolic activity on muscle, strongly dissociated from the androgenic activity on prostate after oral dosing. (-)-**18a** has very good pharmacokinetic properties, including bioavailability in rat ($F > 50\%$), and is currently under evaluation in phase I clinical trials.



INTRODUCTION

The androgen receptor (AR), which belongs to the nuclear receptor superfamily, is activated by endogenous androgens, such as testosterone (T) and its metabolite dihydrotestosterone (DHT). Modulation of the AR results in the control of several physiological characteristics, including differentiation and growth of male reproductive organs, as well as effects on hair and skin (androgenic effects). In addition, other tissues such as muscle and bone are also a target for androgens (anabolic effects). Various steroidal AR ligands have been developed, but their usage has been limited because of poor oral bioavailability and a lack of selectivity between anabolic and androgenic effects, leading to risk of serious side effects.¹ Therefore, the concept of a nonsteroidal, selective androgen receptor modulator (SARM) emerged as an attractive target for drug discovery. Our goal was to identify orally available SARMS, potent and efficacious in anabolic effects, while avoiding undesired androgenic activity. A number of nonsteroidal SARMS that are in preclinical or clinical development have been reported to date (Figure 1).² Chemical scaffolds, including bicalutamide derivatives **1**,³ hydantoin compounds **2**,⁴ and quinolinone derivatives **3**,⁵ have revealed potent and efficacious anabolic activity. Recently, we reported the discovery of (*R*)-4-[3,4-dimethyl-2,5-dioxo-4-(4-hydroxyphenyl)imidazolidin-1-yl]-2-(trifluoromethyl)benzonitrile ((*R*)-(+)-**4**) as a new SARM.⁶

This new partial agonist compound, (+)-**4**, displayed tissue selectivity following oral administration in animal models with reduced androgenic effects on prostate as compared to anabolic

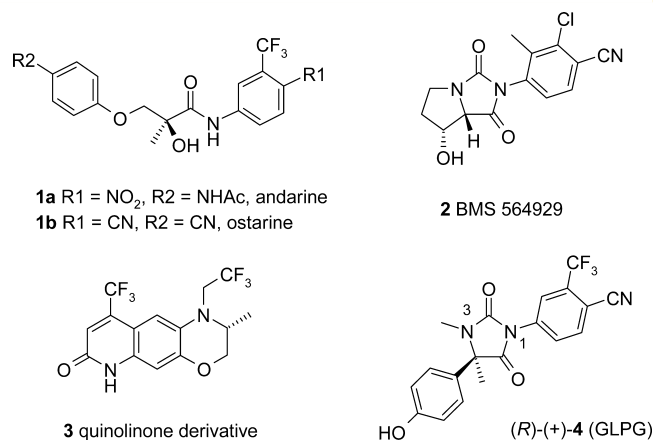
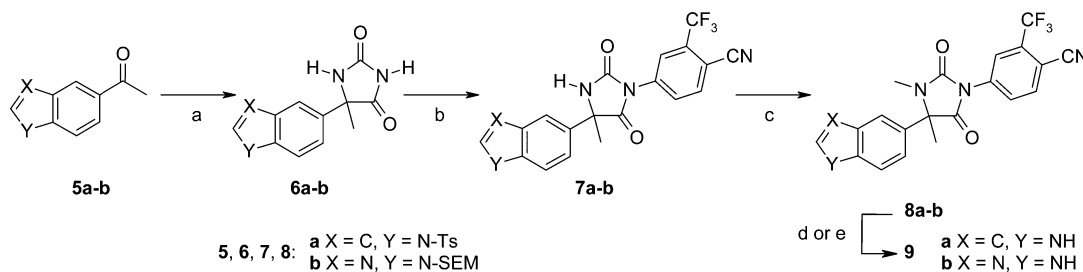


Figure 1. AR ligands.

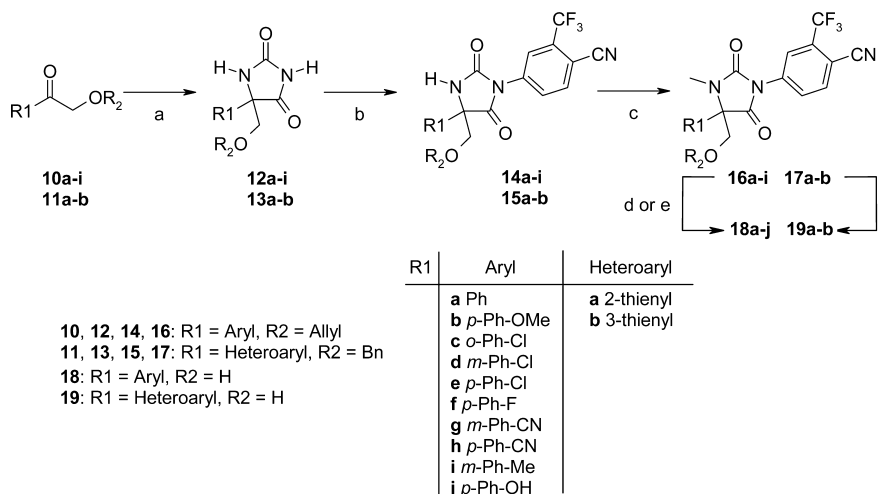
activity on muscle. However, low oral bioavailability⁷ of (+)-**4** ($F < 9\%$ in rat and monkey) prompted us to undertake structure–activity relationship (SAR) studies to maintain the *in vivo* efficacy and the tissue-selective profile of (+)-**4** while significantly increasing oral bioavailability. Many modifications have been made around the hydantoin scaffold, and only a few compounds were identified with the desired *in vivo* profile and good oral bioavailability. Herein, we describe the discovery of (-)-**18a** (GLPG0492), a SARM with tissue differentiation for

Received: February 28, 2012

Published: September 10, 2012

Scheme 1. General Synthesis of 4-Methylhydantoin Analogues (\pm)-9a,b^a

^aReagents and conditions: (a) KCN, (NH₄)₂CO₃·H₂O, EtOH/H₂O (1/1), 60 °C, 18–93 h, 16–100%; (b) 4-bromo-2-(trifluoromethyl)benzoyl cyanide, Cu₂O, DMAc, 130–170 °C, 16–18 h, 18–63%; (c) MeI, NaH, DMF or DMAc, rt, 3 h, 28–100%; (d) Cs₂CO₃, THF/MeOH, 60 °C, 30 min, 73%; (e) HCl 4 N in dioxane, MeOH, 100 °C, 24 h, 86%.

Scheme 2. General Synthesis of 4-Aryl- or 4-Heteroaryl-4-(hydroxymethyl)hydantoin Analogues (\pm)-18a–j and (\pm)-19a,b^a

^aReagents and conditions: (a) KCN, (NH₄)₂CO₃·H₂O, EtOH/H₂O (1/1), 55–80 °C, 8–90 h, 46% to quantitative yield; (b) 4-bromo-2-(trifluoromethyl)benzoyl cyanide, Cu₂O, DMAc, 130–160 °C, 1–48 h, 36–77%; (c) MeI, K₂CO₃, DMF, rt, 2–18 h, 81% to quantitative yield; (d) BF₃·Me₂S, CH₂Cl₂, rt, 2–18 h, 48–87%; (e) *n*-Bu₃SnH, Pd(PPh₃)₄, AcOH, toluene, reflux, 30 min, 48%; (f) Pd(OH)₂/C, cyclohexene, EtOH, 80 °C, 3–48 h, 7–71%.

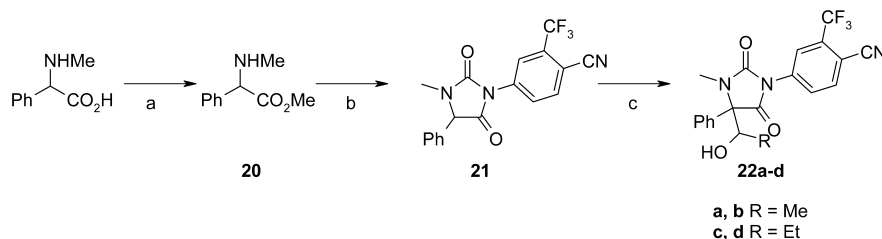
muscle vs prostate and with significant improvement of oral bioavailability (>50%) in the rat. GLPG0492 is currently in phase I clinical trials. The biological and pharmacokinetic (PK) evaluation of this compound will be described.

CHEMISTRY

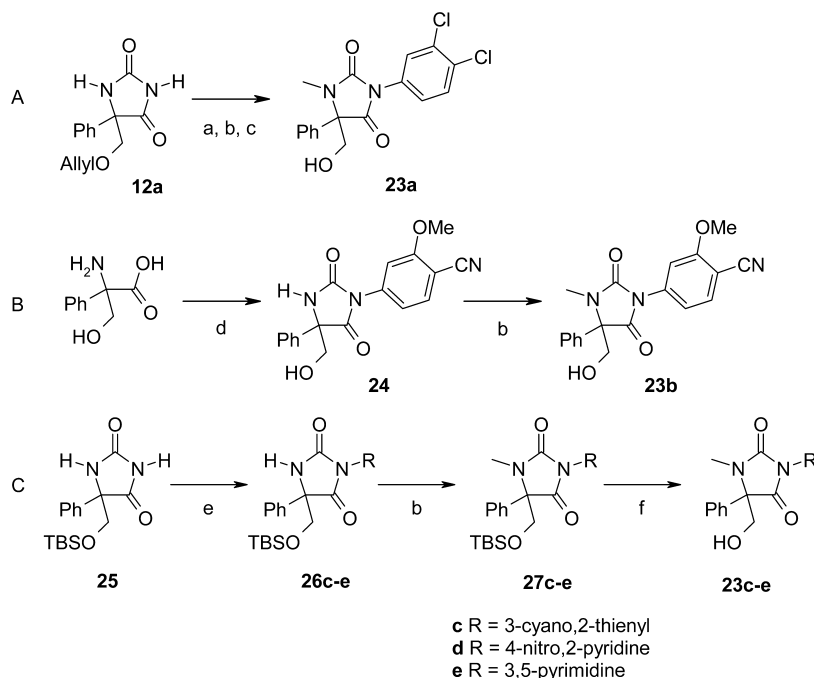
The design of novel SARM compounds was performed to explore five different chemical modifications around the hydantoin scaffold as depicted in Schemes 1–5.

The first series of analogues 9a,b, characterized by replacing the phenol ring with 5-indolyl and 5-benzimidazolyl rings, were prepared as illustrated in Scheme 1. Ketones 5a,b⁸ were condensed with potassium cyanide and ammonium carbonate in a Bucherer–Bergs-type reaction to give the 4-heteroarylhydantoin scaffold 6. Regioselective copper coupling with 4-bromo-2-(trifluoromethyl)benzoyl cyanide was effected at the N1 position to afford the requisite *N*-arylhydantoin 7a,b in low to moderate yield (18–63%). Subsequent *N*-alkylation with methyl iodide in the presence of sodium hydride yielded compounds 8a,b. Finally, targets (\pm)-9a,b were obtained after removal of the tosyl or (2-(trimethylsilyl)ethoxy)methyl (SEM) protecting groups under basic or acidic conditions with 73% or 86% yield, respectively.

As depicted in Scheme 2, the second series of novel templates focused on substituting the 4-methyl group with hydroxyl, as well as replacing the phenol by a panel of different rings. These new analogues, (\pm)-18a–j and (\pm)-19a,b, were obtained starting from protected hydroxymethyl ketones 10a–i and 11a,b using a synthetic route similar to that described in Scheme 1. Appropriate 1-aryl-2-(allyloxy)ethanones⁹ 10a–c,¹⁰ 10d–i,¹¹ and 11a,b¹² employed in this study were prepared in one, two, or three steps from suitable, commercially available compounds. Ketones 10a–i and 11a,b were converted to cyclic 4-aryl- or 4-heteroarylhydantoin 12a–i (50% to quantitative yield) and 13a,b (46–82%) via the Bucherer–Bergs reaction. *N*-arylation with 4-bromo-2-(trifluoromethyl)benzoyl cyanide provided 14a–i (38–71% yield) and 15a,b (36–77%), which were *N*-alkylated to yield compounds 16a–i (88% to quantitative yield) and 17a,b (81–93%). Finally, targets (\pm)-18a,c–i were obtained after removal of the allyl group using boron trifluoride–methyl sulfide complex (in 48–85% yield). Selective deprotection of the allyl group in the presence of the methoxyphenyl ring in compound 16b was carried out with tri-*n*-butyltin hydride to furnish (\pm)-18b (48% yield). On the other hand, nonselective deprotection of 16b with boron trifluoride–methyl sulfide complex provided (\pm)-18j (87%

Scheme 3. General Synthesis of α -Substituted 4-Hydroxymethyl Analogues (\pm)-22a–d^a

^aReagents and conditions: (a) SOCl_2 , MeOH, rt, 48 h, 91%; (b) 4-cyano-3-(trifluoromethyl)phenyl isocyanate, Et_3N , THF, 76%; (c) LiHMDS (1 M in hexanes), THF, -78°C , 10 min, then RCHO, -78°C , 30 min (26–55%).

Scheme 4. Synthesis of *N*-Aryl- and *N*-Heteroaryl-4-hydroxymethyl Analogues (\pm)-23a–e^a

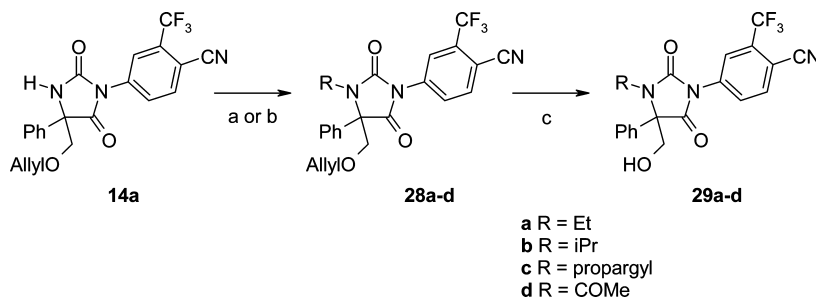
^aReagents and conditions: (a) 1,2-dichloro-4-iodobenzene, Cu_2O , DMAc, 160°C , 3 h, 45%; (b) MeI, K_2CO_3 , DMF, rt, 5–18 h, 13–94% for B and C pathways; (c) $\text{BF}_3 \cdot \text{Me}_2\text{S}$, CH_2Cl_2 , rt, 5 h, 71% (over two steps for A pathway); (d) 4-cyano-3-methoxyphenyl isocyanate, NaOH (1 N), H_2O , rt, 18 h, then HCl (12 N), 120°C , 3 h, 38%; (e) RBr, Cu_2O , DMAc, microwave, 160°C , 50–100 min, **26c** (21%), **26e** (34%) or RBr, K_2CO_3 , DMF, microwave, 150°C , 10 min, **26d** (31%); (f) HCl (4 N in dioxane), rt, 48 h, 33–77%.

yield). The *O*-benzyl group was removed via catalytic hydrogenation to afford (\pm)-**19a,b** (in 7–71% yield).

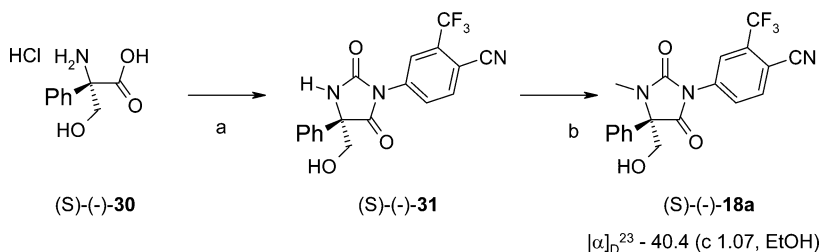
On the basis of compound (\pm)-**18a**, various α -substituted 4-hydroxymethyl analogues (\pm)-**22a–d** constituting a third series were synthesized as shown in Scheme 3 by deprotonation–hydroxyalkylation of the carbon of the hydantoin ring. Methyl esterification of commercially available 2-(methylamino)-2-phenylacetic acid was carried out to give **20** in 91% yield. Immediate cyclization with freshly prepared 4-cyano-3-(trifluoromethyl)phenyl isocyanate provided phenylhydantoin **21** in good yield (76%). Lithiation of **21** with lithium bis(trimethylsilyl)amide at -78°C was followed by addition of acetaldehyde/propionaldehyde to provide a mixture of diastereoisomeric compounds (\pm)-**22a,b**/ (\pm) -**22c,d**, respectively, which were separated by silica gel chromatography, but the relative configuration of the diastereoisomers was not determined (**22a** (15%), **22b** (11%)/**22c** (26%), **22d** (29%)).

With further novel templates, structure modification focused on replacing the (trifluoromethyl)benzonitrile ring (N1 position) with a panel of aryl or heterocyclic rings. Scheme 4

outlines three different ways (A–C) to prepare new compounds of the fourth series. Elaboration of compound (\pm)-**23a** (Scheme 4A) proceeded as outlined in Scheme 2 starting from **12a** using 1,2-dichloro-4-iodobenzene instead of 4-bromo-2-(trifluoromethyl)benzonitrile (32% overall yield). Freshly prepared 4-cyano-3-methoxyphenyl isocyanate⁶ was cyclized with 2-amino-3-hydroxy-2-phenylpropanoic acid¹³ to give **24** in moderate yield (38%). *N*-methylation provided (\pm)-**23b** (Scheme 4B, 13% yield). To introduce heteroaryl rings, intermediate **25**¹⁴ was prepared starting from 2-hydroxyacetophenone in two steps (92% overall yield): (i) protection of the hydroxy function with *tert*-butyldimethylsilyl (TBS); (ii) cyclization under Bucherer–Bergs conditions. A coupling reaction conducted under microwave irradiation with a panel of bromoheteroaryls then furnished **26c–e** (21–34%). *N*-methylation provided **27c–e** (34–94%), which were deprotected under acidic conditions to give (\pm)-**23c–e** in yields ranging from 33% to 77% (Scheme 4C). Both allyl and TBS protecting groups can be used, and there is no specific reason to use one or the other to generate compounds **23**.

Scheme 5. General Synthesis of *N*-Alkyl- and *N*-Acyl-4-hydroxymethyl Analogues (\pm)-29a–d^a

^aReagents and conditions: (a) RX, K₂CO₃, DMF, rt, 4–5 h 70–90%; (b) MeCOCl, TEA, CH₂Cl₂, rt, 18 h, 61%; (c) BF₃·Me₂S, CH₂Cl₂, rt, 4–22 h, 51–80%.

Scheme 6. Determination of the Absolute Configuration of Compound 18a^a

^aReagents and conditions: (a) 4-cyano-3-(trifluoromethyl)phenyl isocyanate, NaOH (0.5 N), dioxane, rt, 18 h, then HCl (12 N), 120 °C, 90 min, 57% over two steps; (b) Me₂SO₄, K₂CO₃, DMAC, rt, 15 h, 72%.

A final series of analogues was synthesized to explore N3 substitution (Scheme 5). Hydantoin 28a–d were prepared in good yields (61–90%) from common intermediate 14a by treatment with alkyl halides or acetyl chloride in the presence of base. A final deprotection step furnished targets (\pm)-29a–d (51–80%).

Generally, the target molecules were prepared as racemates. Selected compounds were separated into individual enantiomers by chiral HPLC.¹⁵ Thus, (–)-18a and (+)-18a were initially isolated from a racemic mixture by means of chiral preparative HPLC in excellent yields ((–)-18a, $[\alpha]_{\text{D}}^{23} = -40.8$ (c 1, EtOH), 48% yield; (+)-18a, $[\alpha]_{\text{D}}^{23} = +41.1$ (c 1, EtOH), 46.5% yield). To unequivocally assign the absolute configurations (Scheme 6), enantiopure compound 18a was prepared from enantiopure (S)-(-)- α -(hydroxymethyl)phenylglycine hydrochloride (30), obtained by fractional crystallization¹⁶ using (–)-cinchonidine.

Enantiopure hydrochloride 30 reacted with 4-cyano-3-(trifluoromethyl)phenyl isocyanate to give the urea intermediate, which cyclized in acidic conditions to give hydantoin 31 in 57% yield over two steps. Final N-alkylation provided compound 18a in 72% yield with an enantiomeric excess of >95% (determined by chiral HPLC). The measurement of optical rotation gave a negative value ($[\alpha]_{\text{D}}^{23}((\text{S})\text{-18a}) = -40.4$ (c 1, EtOH)), thus assigning the S configuration to the more active enantiomer (–)-18a. This result is in agreement with the docking studies below and also with the previously described hydantoin (\pm)-4 configuration, which has been confirmed upon cocrystallization with the ligand binding domain (LBD) of the AR.⁶ The asymmetric synthesis of compound (S)-(-)-18a has been carried out on a 100 g scale from (2*R*,4*S*)-5-oxo-2,4-diphenyloxazolidine-3-carboxylic acid benzyl ester using Seebach methodology, and the dedicated optimization will be reported soon. This asymmetric synthesis gave an additional

confirmation of the absolute configuration of the active compound 18a.

RESULTS AND DISCUSSION

In Vitro. The strategic goal was to identify compounds displaying a strong dissociation between anabolic effects on muscle and/or the bone (requiring a strong agonist activity) versus effects on prostate (where the compound should ideally be an antagonist or a very weak agonist). This goal translates to the identification of a partial agonist using an in vitro transcriptional assay (Hela cell line transfected with hAR and an androgen responsive element (ARE) coupled with luciferase) as described in our previous work (preceding paper in this issue).⁶ A conceptual framework for classifying activity was chosen to help guide the SAR of the series and identify potent compounds (potency parameter). For the SARM profile, evaluation of the partial agonism property with the molecular efficacy parameter indicated if the compounds prepared are suitable for further in vivo evaluation. Potency and molecular efficacy were generated on the basis of the Monod–Wyman–Changeux model,¹⁷ which was used heuristically to identify in vitro most promising compounds to be tested in the in vivo Hersherberger model. Dose–response curves have been generated, crossing a range of DHT concentrations with a range of concentrations for each SARM compound, using a Schild-type curve-shift paradigm approach.⁶ In this transcriptional assay, the in vitro potency value for DHT alone is 8 nM, and we observed modifications of the DHT dose–response curve when different concentrations of the SARM compound were added. We showed that this model provided an excellent framework for evaluation of partial agonism, leading to potency and molecular efficacy data that translate to in vivo activity and tissue selectivity. This is exemplified by using the reference compound ostarine (1b), which progressed in clinical develop-

ment and is known for its tissue-selective anabolic effect. In our assay, **1b** is potent (1.5 nM) with a molecular efficacy of 60, which indicates partial agonism in our conditions. Within the hydantoin series, we identified compound **4**,⁶ which exhibited the in vitro partial agonist profile (potency 0.9 nM/molecular efficacy 132), leading to a potent in vivo activity on levator ani (LA) muscle in an orchidectomized (ORX) rat model (A_{50} = 0.5 mg/kg/day). This compound showed a strong dissociation (factor of 140) between the muscle and the prostate. The SAR indicated that the presence of the phenol substituent on the hydantoin ring is critical for both the potency and the partial agonism, the corresponding unsubstituted phenyl ring being an antagonist (potency 37 nM/molecular efficacy 3). Thus, the phenol group gives a clear advantage in terms of the overall SARM profile; however, it is less favorable in terms of oral exposure, especially due to the potentially direct phase II conjugation process (sulfation, glucuronidation, ...) and clearance. Actually, hydantoin (+)-**4** displayed poor oral bioavailability⁷ (less than 9% both in rat and in monkey), which is not compatible with clinical development. The goal of the lead optimization program was thus to keep the partial agonism in vitro profile while improving oral bioavailability.

We used our recent crystallographic study¹⁸ of hydantoin (+)-**4** bound to the hAR LBD, which showed key interactions between the diarylhydantoin and the binding pocket of the receptor. Initially focusing on the interaction between the hydroxyl group of the phenol and His874, we thought to retain the interaction with various bioisosteres of the phenol, with the goal to retain a H-bond interaction with His874. However, the prepared compounds (for example, OH replaced by NH₂, CH₂OH, and CH(CH₃)OH) turned into full antagonists. Similarly, benzimidazole (\pm)-**9b** displayed an antagonist profile. Surprisingly, the indole analogue (compound (\pm)-**9a** with one nitrogen to carbon replacement when compared to benzimidazole (\pm)-**9b**) restored the desired partial agonist profile initially observed with the phenol (\pm)-**4**, with a molecular efficacy of 35, albeit with a 70-fold weaker in vitro potency (70 nM).

Starting from the X-ray costructure of compound **4** within the AR LBD,¹⁸ docking studies confirmed the interaction between the NH of (\pm)-**9a** and His874 in the AR LBD (Figure 2), thus validating the bioisosteric replacements of the phenol moiety. In addition, the remaining carbon atoms of the five-membered ring were predicted to interact with nearby

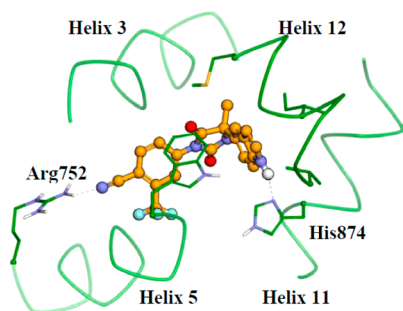


Figure 2. Simplified view of the binding site showing how (*R*)-**9a** (orange carbons) would interact with the AR LBD (green tube and carbons), highlighting the two H-bonds with Arg752 and His874. Residues interacting through a hydrophobic effect with the indole are simply shown as sticks (Trp741 on helix 5, Met895, Ile899, and Val903 on helix 12).

hydrophobic residues Trp741 of helix 5 and Met895, Ile899, and Val903 of helix 12. Interestingly, Bohl et al. theorize that interacting with residues in this region is crucial in the balance between agonist and antagonist properties.¹⁹ The benzimidazole analogue (\pm)-**9b**, which is significantly more hydrophilic than the phenol or the indole, is likely to disturb this region and cause loss of the partial agonist property, yielding a pure antagonist. This is in line with the model whereby antagonism can be the result of a displacement of helix 12 over the coactivator binding pocket as first shown for raloxifene in the estrogen receptor.²⁰

As shown in Table 1, replacement of the phenol moiety by the indole led to a 45-fold decrease in potency (potency 70

Table 1. In Vitro Activity and Absolute Oral Bioavailability for 4-Methyldiarylhydantoin Analogues on hAR (Hela Cells)

compd	R	chiral center	in vitro potency (nM)	in vitro molecular efficacy	F^a (%)
DHT			8	4000	
TP			1.5	600	
(\pm)- 4	<i>p</i> -PhOH	RS	1.6	114	1.5
(+)- 4	<i>p</i> -PhOH	R	0.9	132	9
(\pm)- 9a	indole	RS	70	35	19
(\pm)- 9b	benzimidazole	RS	40	1	100

^a F was determined in rats with a single oral dose of 10 mg/kg in EtOH/PEG400/H₂O (1/79/20, v/v/v) vehicle and a single iv dose of 3 mg/kg in DMSO/PEG400/H₂O (1/65/34, v/v/v).

nM) vs that of the phenol hydantoin (\pm)-**4**. Therefore, the hydantoin indole was not the optimal compound. On the other hand, oral bioavailability was significantly improved with the indole and the benzimidazole substituents on the hydantoin (**9a**, F = 19%, and **9b**, F = 100%, respectively) compared to the phenol ((\pm)-**4**, F < 9%). These results confirmed that although the phenol moiety is important for the partial agonism profile, it also turns out to be a key issue for PK. Therefore, the proposal was to identify active partial agonists devoid of the phenol group, thereby potentially leading to improved PK properties suitable for drug development.

Our strategy to remove the phenol moiety and overcome the lack of bioavailability was to use and pick an additional interaction with the AR LBD and remove the phenol interaction with His874. Analysis of the X-ray structure of DHT within the AR LBD indicates an H-bond interaction between the hydroxyl group of DHT and Asn705. Starting from the X-ray crystal of compound (+)-**4**, a new series was designed around the hydantoin scaffold to target the formation of a H-bond with the Asn705 residue. As part of this work a new series of compounds were synthesized, including (\pm)-**18a** and (\pm)-**18j**, which bear a hydroxymethyl group on the hydantoin scaffold to interact with Asn705.

The docking studies indicate interactions of analogues (\pm)-**18a** with Asn705 and Arg752 and (\pm)-**18j** with Asn705, Arg752, and His874 (Figure 3). As proposed earlier,¹⁹ such ligands are capable of stabilizing an agonist conformation of the AR LBD by tightening helices 3, 5, 11, and 12 together through

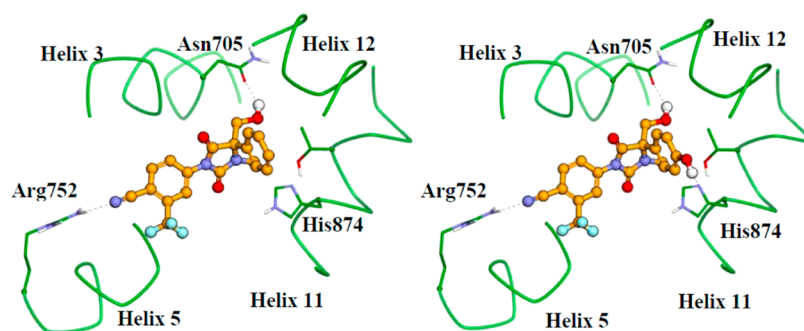
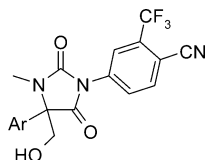


Figure 3. Simplified view of the binding site showing how (*S*)-**18a** (left) and (*S*)-**18j** (right) would interact with the AR LBD (green tube and carbons), highlighting the two H-bonds with Arg752 and Asn705 and the supplementary interaction of (*S*)-**18j** with His874.

both hydrogen bonding and van der Waals contacts. The modeling studies were confirmed by the *in vitro* activities.

The *in vitro* activity and absolute oral bioavailability of these compounds are shown in Table 2. Despite the additional

Table 2. In Vitro Activity and Absolute Oral Bioavailability for 4-(Hydroxymethyl)diarylhydantoin Analogues (\pm)-18a,b,j** (*-*)-**18a**, and (*+*)-**18a****



compd	Ar	chiral center	<i>in vitro</i> potency (nM)	<i>in vitro</i> molecular efficacy	F^a (%)
(\pm)- 18a	Ph	<i>RS</i>	12	78	63
(<i>-</i>)- 18a	Ph	<i>S</i>	13	160	56
(<i>+</i>)- 18a	Ph	<i>R</i>	1250	7	NT ^b
(\pm)- 18b	<i>p</i> -PhOMe	<i>RS</i>	30	17	25
(\pm)- 18j	<i>p</i> -PhOH	<i>RS</i>	0.9	60	15

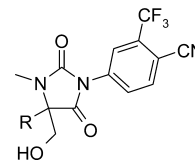
^a F was determined in rats with a single oral dose of 10 mg/kg in EtOH/PEG400/H₂O (1/79/20, v/v/v) vehicle and a single *iv* dose of 3 mg/kg in DMSO/PEG400/H₂O (1/65/34, v/v/v). ^bNT = not tested.

interaction of the $-\text{CH}_2\text{OH}$, hydantoin (\pm)-**18j** kept a high potency similar to that of (\pm)-**4** (potency 0.9 and 1.6 nM, respectively) and maintained a partial agonist profile (molecular efficacy 60 and 114, respectively). However, where the phenol group is not present, (\pm)-**18a** also displayed a partial agonism profile (molecular efficacy 78) with good potency (12 nM). This was the first time we identified a partial agonist within the hydantoin series with a compound lacking an interaction with His874 (through the phenol), knowing that compounds without the phenyl group usually display an antagonist profile. This surprising finding opened new perspectives to solve the PK issues, in particular the bioavailability, while resulting in potent compounds with a partial agonism profile. The (hydroxymethyl)hydantoin compound (\pm)-**18a** retained a partial agonist profile (molecular efficacy 78), which was clearly due to a specific effect of the hydroxymethyl substituent as the corresponding compound bearing the methyl substituent gave an antagonist profile (potency 37 nM, molecular efficacy 3).⁶ The racemic mixture (\pm)-**18a** has been resolved to its pure enantiomers by chiral chromatography. The (*S*)-(*-*)-**18a** isomer proved to be as active as the racemate, while the (*R*)-

(*+*)-**18a** isomer is almost inactive. These data are in good agreement with the docking studies. Direct binding of (*S*)-(*-*)-**18a** to the AR receptor was also measured and was found to be in a range similar to that in the transcriptional assay (21 nM vs 13 nM).

Overall, introduction of the hydroxymethyl substituent on the hydantoin ring led to retention of potency, possibly from the additional interaction with Asn705, and maintained a partial agonism profile, with modulation of potency depending on the aryl group substituent (**18a–j**, Tables 2 and 3). To further

Table 3. In Vitro Activity and Absolute Oral Bioavailability for 4-(Hydroxymethyl)diarylhydantoin Analogues (\pm)-18c–i** and (\pm)-**19a,b****



compd	R	chiral center	<i>in vitro</i> potency (nM)	F^a (%)
(\pm)- 18a	Ph	<i>RS</i>	12	63
(\pm)- 18c	<i>o</i> -PhCl	<i>RS</i>	60	NT ^b
(\pm)- 18d	<i>m</i> -PhCl	<i>RS</i>	5	NT ^b
(\pm)- 18e	<i>p</i> -PhCl	<i>RS</i>	8	99
(\pm)- 18f	<i>p</i> -PhF	<i>RS</i>	11	87
(\pm)- 18g	<i>m</i> -PhCN	<i>RS</i>	60	NT ^b
(\pm)- 18h	<i>p</i> -PhCN	<i>RS</i>	150	NT ^b
(\pm)- 18i	<i>m</i> -PhMe	<i>RS</i>	40	NT ^b
(\pm)- 19a	2-thienyl	<i>RS</i>	150	NT ^b
(\pm)- 19b	3-thienyl	<i>RS</i>	133	NT ^b

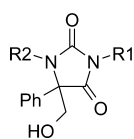
^a F was determined in rats with a single oral dose of 10 mg/kg in EtOH/PEG400/H₂O (1/79/20, v/v/v) vehicle and a single *iv* dose of 3 mg/kg in DMSO/PEG400/H₂O (1/65/34, v/v/v). ^bNT = not tested.

explore the impact of the hydroxymethyl substituent, we synthesized substituted 4-hydroxymethyl analogues (\pm)-**22a–d** as diastereoisomers (methyl and ethyl substituents). However, (\pm)-**22a–d** are antagonists, confirming that this region of the molecule also plays a critical role in the agonism/antagonism profile of the compounds. Therefore, it was decided to keep the hydroxymethyl as a critical substituent on the hydantoin to conserve the desired partial agonist profile.

Critically, the bioavailability of the new (hydroxymethyl)-hydantoin series was evaluated. Conversion of the methyl to hydroxymethyl on the hydantoin scaffold along with removal of the hydroxyl of the phenol (i.e., (*+*)-**4** vs (\pm)-**18a**) significantly

improved bioavailability: (\pm)-**18a** exhibited a much better bioavailability of 63% in rat. Comparison of the two phenol compounds **4** and (\pm)-**18j** shows that (\pm)-**18j** has a slightly improved oral bioavailability (9% vs 15%), confirming the deleterious role of the phenol moiety for bioavailability. Therefore, overall, the outcome of the (hydroxymethyl)-hydantoin series was really unexpected and very surprising. We observed that, despite the OH of the phenol being deleted, the potency and the desired partial agonism profile could be retained while resulting in a great improvement in bioavailability. Thus, (\pm)-**18a** fulfilled the key criteria of potency, partial agonism, and good oral bioavailability and was selected for further improving the SAR of the remaining hydantoin substituents as indicated in Tables 3 and 4.

Table 4. In Vitro Activity and Absolute Oral Bioavailability for 4-(Hydroxymethyl)diarylhydantoin Analogues (\pm)-23a**,**b** and (\pm)-**29a**–**d****



compd	R1	R2	chiral center	in vitro potency (nM)	F ^a (%)
(\pm)- 18a	3-CF ₃ -4-CNPh	Me	RS	12	63
(\pm)- 23a	3-Cl-4-ClPh	Me	RS	60	NT ^b
(\pm)- 23b	3-OMe-4-CNPh	Me	RS	60	NT ^b
(\pm)- 29a	3-CF ₃ -4-CNPh	Et	RS	7	76
(\pm)- 29b	3-CF ₃ -4-CNPh	iPr	RS	20	NT ^b
(\pm)- 29c	3-CF ₃ -4-CNPh	propargyl	RS	40	NT ^b
(\pm)- 29d	3-CF ₃ -4-CNPh	COMe	RS	150	NT ^b

^aF was determined in rats with a single oral dose of 10 mg/kg in EtOH/PEG400/H₂O (1/79/20, v/v/v) vehicle and a single iv dose of 3 mg/kg in DMSO/PEG400/H₂O (1/65/34, v/v/v). ^bNT = not tested.

As depicted in Table 3, investigations on modifications of the aromatic substituent close to the hydroxymethyl group were conducted. The SAR revealed phenylhydantoin (\pm)-**18a** and substituted phenylhydantoin (\pm)-**18c**–**i** are more potent than thiophenes (\pm)-**19a**,**b**, which led to a significant loss in potency.

Substitution on the phenyl group indicated that introduction of halogen atoms in the meta or para position ((\pm)-**18d**–**f**) induced no real change in potency (5–11 nM). The *o*-chlorophenyl analogue (\pm)-**18c** resulted in a decrease of activity (potency 60 nM). The electron-withdrawing cyano groups in (\pm)-**18g**,**h** decreased potency 5–12-fold compared to that of (\pm)-**18a**. The same observation was made with the *m*-methyl group (potency 40 nM). Although the substitutions depicted in Table 3 did not significantly improve the in vitro profile of compound (\pm)-**18a**, the active compounds identified from this study were evaluated in vivo.

The next study was to define the importance of the aryl ring and substitution at the N1 position. Although it is well-known that variations at this part of nonsteroidal androgen molecules are very limited to retain good affinity for the AR, a number of

analogues, (\pm)-**23a**–**e**, were synthesized and tested in the hAR assay. Replacement of the 4-cyano-3-(trifluoromethyl)phenyl with heterocycles still bearing electron-withdrawing groups for the ability to make a hydrogen bond with Arg752 resulted in analogues (\pm)-**23c**–**e**. These three compounds turned out to be weakly active with an antagonist profile (molecular efficacy <1), suggesting that heterocycles did not correctly orient to interact with the AR LBD. On the other hand, as shown in Table 4, the potency of the 4-cyano-3-methoxyphenyl analogue (\pm)-**23b** and more surprisingly of the 3,4-dichlorophenyl analogue (\pm)-**23a** was reduced only 5-fold (potency 60 nM), similarly to previous observations.⁶

Analogues (\pm)-**29a**–**d** were prepared in which the *N*3-methyl group was replaced. Ethyl-substituted (\pm)-**29a** gave similar potency (7 nM), and both isopropyl ((\pm)-**29b**) and propargyl ((\pm)-**29c**) analogues resulted in a slight decrease in potency (20 and 40 nM, respectively). Acylation as in (\pm)-**29d** led to further loss of activity (potency 150 nM) and turned the profile to full antagonism (molecular efficacy 2).

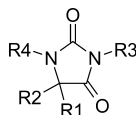
In Vivo. As several of these racemic compounds displayed partial agonist profiles in vitro with potencies close to that of (\pm)-**4**, we evaluated the ability to stimulate muscle anabolism vs prostate growth in the Hershberger model of ORX rats. Castrated rats were left untreated for one week and then orally treated for four days with test compound (10 mg/kg/day). The weight of the LA muscle was considered a marker of anabolic activity, whereas the weight of the ventral prostate (VP) was regarded as a marker of androgenic activity.²¹ Results of these experiments are shown in Table 5.

At the dose of 10 mg/kg/day, compounds (\pm)-**18a**,**d**,**g**, (\pm)-**23a**, and (\pm)-**29a**–**c** restored the weight of LA to near that of sham control animals while the VP weights remained far below those of intact animals, thereby indicating dissociation of anabolic and androgenic effects in accordance with the in vitro activities of a potent partial agonist. Compounds (\pm)-**18c**,**h**,**i** displayed weaker in vivo activity on LA, in line with weaker in vitro potency. Despite the fact that (\pm)-**18j** was the most active compound in vitro (potency 0.9 nM), it was not the best anabolic compound (even at 30 mg/kg/day). This might be explained by its low oral bioavailability. In addition, compound (\pm)-**18j** did not show a great dissociation between anabolic and androgenic effects. Finally, methoxyphenyl (\pm)-**18b** resulted in the highest anabolic effect among all these molecules, albeit not dissociated from androgenic activity. These data are not in line with the in vitro profile of (\pm)-**18b** but can be explained by in vivo demethylation of the methoxy group of (\pm)-**18b** to lead to the phenol (\pm)-**18j**, which is potent, but not very well dissociated between muscle and prostate.

The racemate (\pm)-**18a** and the pure enantiomer (*S*)-(-)-**18a** completely reverted the muscle wasting in ORX rats at 10 mg/kg/day following oral administration; no further increase was observed with the higher dose of 30 mg/kg/day. Interestingly, the maximum activity observed on prostate (26%) was achieved at the dose of 10 mg/kg/day. Thus, the maximum effect on LA muscle was reached at a dose displaying a weak activity on VP.

To further explore the anabolic potency and selectivity of (*S*)-(-)-**18a**, and compare them to those of TP, a wide dose range experiment was performed in the same Hershberger model on ORX male rats (castrated rats left untreated for one week and then orally treated for four days with (*S*)-(-)-**18a**, Figure 4). Dose–response curves for LA and VP in response to TP were almost superimposable, showing A₅₀ = 0.30 and 0.20 mg/kg/day, respectively. On the contrary, (*S*)-(-)-**18a** showed

Table 5. In Vivo Activity for a Panel of Hydantoin Analogues



compd ^a	R1	R2	R3	R4	anabolic activity(LA) (%)	androgenic activity(VP) (%)
TP ^b					99	73
(±)-4	Me	<i>p</i> -PhOH	3-CF ₃ -4-CNPh	Me	68/89 ^c	8/16 ^c
(<i>R</i>)-(+)-4	Me	<i>p</i> -PhOH	3-CF ₃ -4-CNPh	Me	44/77 ^c	12/26 ^c
(±)-18a	CH ₂ OH	Ph	3-CF ₃ -4-CNPh	Me	101/96 ^c	13/14 ^c
(<i>S</i>)-(-)-18a	CH ₂ OH	Ph	3-CF ₃ -4-CNPh	Me	101/106 ^c	24/26 ^c
(±)-18b	CH ₂ OH	<i>p</i> -PhOMe	3-CF ₃ -4-CNPh	Me	130 ^c	95 ^c
(±)-18c	CH ₂ OH	<i>o</i> -PhCl	3-CF ₃ -4-CNPh	Me	26	7
(±)-18d	CH ₂ OH	<i>m</i> -PhCl	3-CF ₃ -4-CNPh	Me	66	16
(±)-18e	CH ₂ OH	<i>p</i> -PhCl	3-CF ₃ -4-CNPh	Me	35	0
(±)-18g	CH ₂ OH	<i>m</i> -PhCN	3-CF ₃ -4-CNPh	Me	84	26
(±)-18h	CH ₂ OH	<i>p</i> -PhCN	3-CF ₃ -4-CNPh	Me	12	11
(±)-18i	CH ₂ OH	<i>m</i> -PhMe	3-CF ₃ -4-CNPh	Me	24	0
(±)-18j	CH ₂ OH	<i>p</i> -PhOH	3-CF ₃ -4-CNPh	Me	82 ^c	55 ^c
(±)-23a	CH ₂ OH	Ph	3-Cl-4-ClPh	Me	96	23
(±)-29a	CH ₂ OH	Ph	3-CF ₃ -4-CNPh	Et	112	59
(±)-29b	CH ₂ OH	Ph	3-CF ₃ -4-CNPh	iPr	109	60
(±)-29c	CH ₂ OH	Ph	3-CF ₃ -4-CNPh	propargyl	96	43

^aAll the test compounds were administered orally with a dose of 10 mg/kg/day. ^bTestosterone propionate (TP) was administered subcutaneously at 1 mg/kg/day. ^cTest compounds were administered orally with a dose of 30 mg/kg/day.

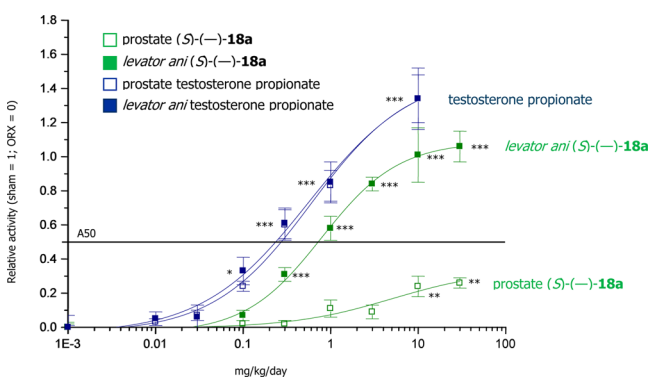


Figure 4. Comparison of the anabolic vs androgenic activities of (*S*)-(-)-18a (GLPG0492) and testosterone propionate in ORX rats. $A_{50} = AD_{50}$, dose displaying 50% activity on levator ani or ventral prostate. Student's *t* test (vs ORX): *, $p < 0.05$; **, $p < 0.01$; ***, $p < 0.001$.

a clear dissociation between anabolic and androgenic effects; the dose displaying 50% activity on LA was 0.75 mg/kg/day, while at the maximum 30% activity can be achieved on VP at the highest dose tested (30 mg/kg/day). This clearly demonstrated the tissue selectivity of LA vs VP for (*S*)-(-)-18a, thereby leading to its classification as an SARM, with a promising preclinical safety profile (muscle vs prostate) for a potential treatment for cachexia.

Dissociation between LA muscle and VP has also been evaluated in a longer model. Castrated rats at the age of seven weeks were treated with (*S*)-(-)-18a by the oral route for three months in a prophylactic setting at the dose of 10 mg/kg/day. Normalizing sham-operated rat at 100% and ORX rat at 0%, we observed in the treated group that the LA weight was fully restored (117%), at a level similar to that of the sham-operated group. Conversely, the increase in prostate weight in rats treated with (*S*)-(-)-18a was much lower (25%), with the prostate weight closer to that of the ORX group than the sham-

operated group. This indicates that dissociation observed in the short-term model is maintained after long-term treatment with 10 mg/kg/day of compound (*S*)-(-)-18a by the oral route.

The PK profile of (*S*)-(-)-18a, after intravenous (iv) and oral (po) routes to Sprague–Dawley male rats, is shown in Table 6. (*S*)-(-)-18a exhibited good exposure (area under the

Table 6. Pharmacokinetic Profile of (*S*)-(-)-18a (GLPG0492) in Rats after Single Administration

administration ^a	CL (mL/min/kg)	$T_{1/2}$ (h)	V_{dss} (L/kg)	$AUC_{(0-\infty)}$ (ng.h/mL)	<i>F</i> (%)
iv ^b	21.7	1.5	2.5	2362	
po ^c		2.2 ^d		4675 ^d	56

^aTwo groups of three rats received the treatment. ^bSingle iv dose of 3 mg/kg in DMSO/PEG200/H₂O (1/79/20, v/v/v). ^cSingle oral dose of 10 mg/kg in EtOH/PEG200/H₂O (1/79/20, v/v/v). Compound (*S*)-(-)-18a was dissolved in EtOH. PEG400 and H₂O were added. The mixture was stirred and placed in an ultrasound bath to give a lipid solution at 2 mg/mL. ^d $N = 2$ rats.

curve, AUC) after oral and iv administration, moderate clearance (CL; around a third of hepatic blood flow), a medium volume of distribution (V_{dss}), and good bioavailability⁷ ($F = 56\%$). Following extensive safety profiling in vitro and in vivo, (*S*)-(-)-18a was selected as a clinical candidate for the treatment of cachexia under the code GLPG0492.

CONCLUSION

Starting from a hydantoin series represented by compound (±)-4, an extensive plan of structural modifications was undertaken with the goal of maintaining the partial agonist profile of compound (±)-4 while significantly improving the oral bioavailability. Thus, five different modifications around the hydantoin were synthesized and explored, leading to a series of new hydantoins bearing a hydroxymethyl substituent. Un-

expectedly, although the potency compared to that of the reference (\pm)-4 was not improved by these modifications, the effect on the oral bioavailability was profound, thereby opening the way to clinical development of compounds with a partial agonism profile. Several compounds around the (hydroxymethyl)hydantoin series induced transcriptional activity of the hAR at nanomolar concentrations in vitro. Partial agonism observed in vitro translated to tissue selectivity of muscle vs prostate in vivo after oral administration in a castrated rat model. Particularly, (S)-(-)-18a maintained levator ani muscle weight with potency similar to that of testosterone while causing only a weak stimulation of the prostate. This clear dissociation between anabolic and androgenic end points in vivo is representative of an SARM. The discovery of this (hydroxymethyl)diarylhydantoin core constitutes a significant advance in the search for efficient and highly tissue-selective nonsteroidal SARMs. The promising compound (S)-(-)-18a (GLPG0492) is now undergoing phase I clinical trials.

EXPERIMENTAL SECTION

Unless otherwise stated, all procedures were performed under a nitrogen atmosphere using anhydrous solvents purchased from commercial sources. Commercially available starting materials and reagents were used as received without further purification. Thin-layer chromatography was performed using precoated Merck silica gel 60 F254 plates, visualized under UV light or after staining by spraying a solution of 20% phosphomolybdic acid in ethanol and then heating. Preparative chromatography was conducted over Merck silica gel 60 (0.040–0.063 mm). All ^1H NMR spectra were recorded using a Bruker DPX (300 MHz) or Advance (400 MHz) spectrometer, in solution in the deuterated solvent mentioned; chemical shifts are expressed in parts per million as a δ value relative to the shift of the tetramethylsilane used as a reference. LC/MS was performed on a Waters HPLC instrument with a 2996 photodiode array detector coupled to an LCT TOF mass spectrometer with electrospray ionization. HPLC method was as follows: column used, Waters Xterra RP18 (3.5 μm , 50 \times 2.1 mm i.d.); solvents, (A) water + 0.01% of formic acid and (B) CH_3CN + 0.01% of formic acid; gradient method, from 95/5 A/B at time 0 to 100% B after 4 min, then 100% B for 3 min. The purity of the described compounds was >98% according to HPLC analysis. Melting points were determined on a Kofler block and are uncorrected. Optical rotations ($[\alpha]_D^{25}$) were recorded on a Propol polarimeter. Specific rotations are given as degrees per decimeter, and the concentrations c are reported as grams per 100 mL of the specific solvent and were recorded at 23 $^\circ\text{C}$.

Method A is protection with allyl bromide following the protocol described in the literature.¹⁰

Method B is a Bucherer–Bergs reaction. To a solution of 1-heteroarylethanone, 1-aryl-2-(allyloxy)ethanone, or 1-heteroaryl-2-(benzyloxy)ethanone in ethanol/water (50/50) were added potassium cyanide and ammonium carbonate. The mixture was heated at 55–80 $^\circ\text{C}$ for 8–93 h. The reaction mixture was diluted with water and extracted with ethyl acetate. The organic solution was washed with a saturated aqueous sodium chloride solution, then dried over sodium sulfate, and evaporated to yield the expected product, which was used in the next step without purification.

Method C is a copper coupling reaction. To a solution of imidazolidine-2,4-dione in dimethylacetamide were added copper(I) oxide and 4-bromo-2-(trifluoromethyl)benzotrile. The mixture was heated at 130–170 $^\circ\text{C}$ for 1–48 h. At rt, the mixture was diluted with a 50% aqueous solution of ammonia and extracted with ethyl acetate. The organic layer was dried over sodium sulfate, filtered, and evaporated. The crude product was purified by chromatography over silica gel to provide the expected product.

Method D is an N-alkylation reaction. To a solution of N-arylhydantoin or N-heteroarylhydantoin and potassium carbonate in

DMF was added iodomethane. The mixture was stirred at rt for 2–18 h, evaporated to dryness, diluted with water, and extracted with ethyl acetate. The organic layer was dried over magnesium sulfate, filtered, and evaporated. The crude product was purified by chromatography over silica gel to give the expected product or used in the next step without purification.

Method E is deprotection with trifluoroborane–dimethyl sulfide complex. To a solution of 4-((allyloxy)methyl)-3-alkyl-1-arylimidazolidine-2,4-dione or 4-((allyloxy)methyl)-3-acyl-1-arylimidazolidine-2,4-dione in dichloromethane was added trifluoroborane–dimethyl sulfide complex in dichloromethane. The mixture was stirred at rt for 2–18 h, poured into a saturated aqueous sodium bicarbonate solution, and extracted with ethyl acetate. The organic layer was dried over magnesium sulfate, filtered, and evaporated. The crude product was purified by chromatography over silica gel or crystallized to provide the final target.

4-[2,5-Dioxo-4-(hydroxymethyl)-3-methyl-4-phenylimidazolidin-1-yl]-2-(trifluoromethyl)benzotrile ((\pm)-18a). *Step 1: 1-Phenyl-2-(2-propenyloxy)ethanone (10a).* The title compound was prepared according to method A from 2-hydroxy-1-phenylethanone (3.66 g, 26.9 mmol), allyl bromide (17 mL), calcium sulfate (16.3 g, 120 mmol), and silver(I) oxide (10.8 g, 46.6 mmol) to give 10a as a yellow oil (1.6 g, 33%) after purification on silica gel with 90/10 heptane/ethyl acetate. ^1H NMR (400 MHz, DMSO): δ 4.10 (d, J = 5.4 Hz, 2H), 4.88 (s, 2H), 5.20 (d, J = 10.5 Hz, 1H), 5.31 (dd, J = 1.48 and 17.3 Hz, 1H), 5.91–6.00 (m, 1H), 7.56 (t, J = 7.6 Hz, 2H), 7.68 (t, J = 7.3 Hz, 1H), 7.94 (d, J = 7.3 Hz, 2H).

Step 2: 4-Phenyl-2-(2-propenyloxy)imidazolidine-2,5-dione (12a). The title compound was prepared according to method B from 10a (1.6 g, 9.07 mmol), potassium cyanide (1.2 g, 18.4 mmol), and ammonium carbonate (18.4 g, 191 mmol) in 1/1 EtOH/ H_2O (50 mL). The mixture was heated at 55 $^\circ\text{C}$ for 26 h to yield 12a as a white-yellow solid (1.9 g, 85%) which was used in the next step without purification. ^1H NMR (400 MHz, DMSO): δ 3.53 (d, J = 9.8 Hz, 1H), 3.98 (d, J = 9.8 Hz, 1H), 3.94–4.02 (m, 2H), 5.17 (d, J = 10.5 Hz, 1H), 5.27 (d, J = 17 Hz, 1H), 5.79–5.89 (m, 1H), 7.32–7.41 (m, 3H), 7.55 (d, J = 7.2 Hz, 2H), 8.62 (s, 1H), 10.74 (s, 1H).

Step 3: 4-[2,5-Dioxo-4-phenyl-4-[(2-propenyloxy)methyl]imidazolidin-1-yl]-2-(trifluoromethyl)benzotrile (14a). The title compound was prepared according to method C from 12a (1.85 g, 7.51 mmol), copper(I) oxide (0.644 g, 4.5 mmol), and 4-bromo-2-(trifluoromethyl)benzotrile (1.9 g, 7.51 mmol) in DMAc (4 mL). The mixture was heated at 160 $^\circ\text{C}$ for 3 h, and the crude product was purified by chromatography over silica gel with 80/20 heptane/ethyl acetate to provide 14a as a white amorphous solid (1.9 g, 61%). ^1H NMR (400 MHz, DMSO): δ 3.74 (d, J = 9.8 Hz, 1H), 4.08–4.09 (m, 2H), 4.19 (d, J = 9.8 Hz, 1H), 5.16 (d, J = 11.1 Hz, 1H), 5.24 (d, J = 17.2 Hz, 1H), 5.83–5.93 (m, 1H), 7.41–7.50 (m, 3H), 7.66 (d, J = 7.4 Hz, 2H), 8.00 (d, J = 8.4 Hz, 1H), 8.11 (s, 1H), 8.33 (d, J = 8.4 Hz, 1H), 9.62 (s, 1H). LC/MS (t_R = 3.02 min): m/z 414 (M – H) $^-$.

Step 4: 4-[2,5-Dioxo-3-methyl-4-phenyl-4-[(2-propenyloxy)methyl]imidazolidin-1-yl]-2-(trifluoromethyl)benzotrile (16a). The title compound was prepared according to method D from 14a (1.9 g, 4.58 mmol), iodomethane (0.97 mL, 15.5 mmol), and potassium carbonate (0.75 g, 5.5 mmol) in DMF (4 mL). The mixture was stirred at rt for 4 h to give 16a as a yellow oil (1.9 g, 97%) which was used in the next step without purification. ^1H NMR (400 MHz, DMSO): δ 2.90 (s, 3H), 4.14–4.16 (m, 2H), 4.23 (d, J = 10.1 Hz, 1H), 4.45 (d, J = 10.1 Hz, 1H), 5.19 (d, J = 10.4 Hz, 1H), 5.25 (dd, J = 1.6 and 17.2 Hz, 1H), 5.88–5.98 (m, 1H), 7.48–7.55 (m, 5H), 8.04 (d, J = 8.6 Hz, 1H), 8.17 (s, 1H), 8.37 (d, J = 8.5 Hz, 1H). LC/MS (t_R = 3.08 min): m/z 430 (M + H) $^+$.

Step 5: 4-[2,5-Dioxo-4-(hydroxymethyl)-3-methyl-4-phenylimidazolidin-1-yl]-2-(trifluoromethyl)benzotrile ((\pm)-18a). The title compound was prepared according to method E from 16a (1.9 g, 4.42 mmol) and trifluoroborane–dimethyl sulfide complex (1.5 mL, 14.3 mmol) in dichloromethane (5 mL). The mixture was stirred at rt for 4 h, and the crude product was purified by chromatography over silica gel with 95/5 dichloromethane/ethyl acetate to give the final target 18a as a white crystalline solid (1.5 g, 83%). Mp = 160 $^\circ\text{C}$. ^1H

NMR (400 MHz, DMSO): δ 2.88 (s, 3H), 4.09 (dd, $J = 2.8$ and 5.3 Hz, 1H), 4.44 (dd, $J = 5.8$ and 11.6 Hz, 1H), 5.80 (t, $J = 5.5$ Hz, 1H), 7.45–7.47 (m, 5H), 8.07 (d, $J = 8.5$ Hz, 1H), 8.20 (s, 1H), 8.35 (d, $J = 8.4$ Hz, 1H). ^{13}C NMR (100 MHz, DMSO): δ 26.3, 61.3, 72.2, 107.4, 115.6, 118.6, 121.2, 123.9, 124.0, 126.7, 127.2, 129.4, 129.5, 129.9, 131.3, 131.6, 132.0, 132.3, 133.8, 136.8, 137.0, 154.7, 172.4. LCMS ($t_{\text{R}} = 2.82$ min): m/z 358 ($\text{M} - \text{CH}_2\text{OH}$) $^-$.

Separation of (\pm)-18a by Chiral HPLC. The two enantiomers of (\pm)-18a were separated from a racemic mixture (1.5 g) by chromatography on Chiralcel OD (LC50 Prochrom column), eluting with a 75/25 heptane/2-propanol mixture.¹⁵

(S)-(-)-4-[2,5-Dioxo-4-(hydroxymethyl)-3-methyl-4-phenylimidazolidin-1-yl]-2-(trifluoromethyl)benzotrile ((S)-(-)-18a). The S enantiomer was eluted first. By evaporating the solvent, (S)-(-)-18a was obtained as an amorphous white solid (720 mg of 99.0% pure compound, 48% yield). $[\alpha]_{\text{D}}^{23} = -40.8$ (c 1, EtOH). HPLC (Chiralcel OD, column 250 \times 4.6 mm, heptane/2-propanol (75/25), flow rate 1 mL/min): $t_{\text{R}} = 9.01$ min.

(R)-(+)-4-[2,5-Dioxo-4-(hydroxymethyl)-3-methyl-4-phenylimidazolidin-1-yl]-2-(trifluoromethyl)benzotrile ((R)-(+)-18a). The R enantiomer was eluted second. Further purification in the same conditions followed by evaporation of the solvent provided (R)-(+)-18a (700 mg of 98.1% pure compound, 46.5% yield) as an amorphous white solid. $[\alpha]_{\text{D}}^{23} = +41.1$ (c 1, EtOH). HPLC (Chiralcel OD, column 250 \times 4.6 mm, heptane/2-propanol (75/25), flow rate 1 mL/min): $t_{\text{R}} = 13.24$ min.

Preparation of (S)-(-)-18a Using a Resolution Procedure. (S)-(-)-4-[2,5-Dioxo-4-(hydroxymethyl)-4-phenylimidazolidin-1-yl]-2-(trifluoromethyl)benzotrile ((S)-(-)-31). To a solution of (S)-(-)- α -(hydroxymethyl)phenylglycine hydrochloride (30)¹⁶ (0.54 g, 2.5 mmol) in NaOH (0.5 N, 16 mL, 3.2 mmol) was added a solution of freshly prepared isocyanate (3 \times 0.65 g, 9 mmol total) in dioxane (3 \times 6 mL). The mixture was stirred at rt for 4 h, treated with HCl (12 N, 15 mL), and heated at 120 $^{\circ}\text{C}$ for 90 min. The mixture was evaporated, extracted with ethyl acetate, dried over magnesium sulfate, filtrated, evaporated, and purified on silica gel with 50/50 heptane/ethyl acetate to give 31 (0.54 g, 57%). ^1H NMR (400 MHz, CDCl_3): δ 4.05 (d, $J = 11.5$ Hz, 1H), 4.43 (d, $J = 11$ Hz, 1H), 6.35 (s, 1H), 7.48–7.53 (m, 3H), 7.64–7.66 (m, 2H), 7.93–8.00 (m, 2H), 8.12 (s, 1H). $[\alpha]_{\text{D}}^{23} = -15.2$ (c 1.13, MeOH).

(S)-(-)-4-[2,5-Dioxo-4-(hydroxymethyl)-3-methyl-4-phenylimidazolidin-1-yl]-2-(trifluoromethyl)benzotrile ((S)-(-)-18a). To a solution of (S)-(-)-31 (188 mg, 0.5 mmol) and potassium carbonate (193 mg, 1.4 mmol) in DMAc (5 mL) was added dimethyl sulfate (160 μL , 1.7 mmol). The mixture was stirred at rt for 15 h, evaporated to dryness, diluted with water, and extracted with ethyl acetate. The organic layer was dried over magnesium sulfate, filtered, and evaporated. The crude was purified by chromatography over silica gel with 50/50 heptane/ethyl acetate to give the S enantiomer as an amorphous white solid (140 mg, 72%). $[\alpha]_{\text{D}}^{23} = -40.4$ (c 1, EtOH).

In Vitro Transactivation Assay. The in vitro molecular efficacy has been assessed using a host stable cell line derived from HeLa cells expressing hAR and a reporter gene placed under the transcriptional control of the probasin AREs. This transactivation assay allows the identification of pure agonists (such as testosterone and DHT), partial agonists, and antagonists.

In the Monod–Wyman–Changeux model,¹⁹ the receptor is constantly in interconversion equilibrium between two states (active, A, and inactive, R), and any ligand of the receptor actually has two molecular affinities for the receptor: one for the active state, A (denoted K_{A}), and one for the inactive state, R (denoted K_{R}). The ratio of the affinities of the compound for the two states, $K_{\text{A}}/K_{\text{R}}$, is called the molecular efficacy of the compound. The position of the equilibrium in the absence of ligand is defined by the ratio $[\text{R}]/[\text{A}]$ and is equal to a constant classically denoted L_0 , $L_{[\text{X}]}$ being the value of this ratio in the presence of the ligand at a concentration $[\text{X}]$. Applying the law of mass action to each of the states, $[\text{RX}] = [\text{R}][\text{X}]/K_{\text{R}}$ and $[\text{AX}] = [\text{A}][\text{X}]/K_{\text{A}}$, leads to the key expression $L_{[\text{X}]} = L_0(1 + [\text{X}]/K_{\text{R}})/(1 + [\text{X}]/K_{\text{A}})$. At saturating concentrations of the ligand, a limit value is obtained: $L_{\infty} = L_0K_{\text{A}}/K_{\text{R}}$. This is precisely the equation

separating, in the expression of molecular efficacy, the contribution of the tissue from that of the compound: The molecular efficacy $K_{\text{A}}/K_{\text{R}}$ expresses the way the compound does or does not discriminate between the two states, whereas L_0 determines the contribution of the tissue. Efficacies reported in this paper are the ratio $K_{\text{A}}/K_{\text{R}}$ related to the compound contribution. Applying the law of mass action to each of the two states also leads to the potency equation $1/K_{\text{d}} = L_0/(1 + L_0)(1/K_{\text{R}}) + 1/(1 + L_0)(1/K_{\text{A}})$, expressing that the apparent affinity is simply the harmonic mean of the two molecular affinities, weighed by the initial position of the equilibrium.

We therefore used a Schild-type curve-shift paradigm approach by crossing a range of concentrations of our compound and a range of concentrations of DHT as the reference agonist. We analyzed both the rightward shift of the DHT curve induced by the antagonist activity of our compound and the upward shift of its lower plateau induced by the agonist activity of our compound. To reach the two molecular affinities K_{A} and K_{R} of our SARM compounds, we built the mathematical theoretical behavior of our system with parametrized equations where K_{A} and K_{R} are the parameters identified by fitting the bundle of curves from the curve-shift paradigm as a whole. From K_{A} and K_{R} , potency and molecular efficacy were calculated as indicated.

In Vivo Pharmacology. The selective modulating activity of the compounds was tested in an adapted model of castrated immature young rats which is widely recognized for evaluating the anabolic and androgenic effects of androgens on muscles and on genitalia.^{21b} Castrated rats were left untreated for one week and then treated for four days with test compound. Castration resulted in a rapid atrophy of the VP as well as of the anus-lifting LA muscle. These effects were completely compensated by an exogenous administration of androgens. Stringency of the therapeutic setting is greater than that of the prophylactic setting and allows detection of more potent myotrophic/anabolic compounds. After four days of treatment, the activity of the compound was expressed as a percentage and calculated using the following formula: $(W/\text{BW}(\text{treated}) - W/\text{BW}(\text{ORX})) / (W/\text{BW}(\text{sham}) - W/\text{BW}(\text{ORX})) \times 100$, where W is weight and BW is body weight. The dissociated activity of the test compound was expressed as the ratio between the dose displaying 50% activity (A_{50}) on VP and that displaying 50% activity on LA.

Molecular Modeling. All molecular modeling studies were performed with version 2.0 of the Discovery Studio (DS) platform, available from Accelrys (San Diego, CA). Compounds were sketched, prepared, and converted into 3D by use of the Ligand Preparation protocol. In the objective of docking the prepared compounds, the resolved crystal structure of AR LBD/(+)-4 described in our previous work¹⁸ was protonated at pH 7.4, and hydrogens were reoptimized with the HBUILT routine of CHARMm (CHARMm Momany and Rone force field).²² Prior to removal, (+)-4 was used to define the binding site volume using the cavity detection algorithm available within the interface.²³ Since the AR LBD exhibits a well-defined and buried binding site, no particular edition of the resulting shape was necessary. Docking was performed with LigandFit, resorting to an energy grid calculated with Dreiding²⁴ to interpolate the protein energy fields. Poses were optimized as rigid bodies by 15 iterations of steepest descent and the 10 best reoptimized by 150 iterations of the Broyden–Fletcher–Goldfarb–Shanno (BFGS) minimization routine. Other parameters remained the default values within DS. Lastly, poses were flexibly minimized (DS “Smart minimizer” with a final 1000 iterations of conjugate gradient minimization) and rank ordered with the scoring function LigScore2.²⁵

■ ASSOCIATED CONTENT

Supporting Information

Synthetic procedures for the final targets (\pm)-9a,b, (\pm)-18b–j, (\pm)-19a,b, (\pm)-22a–d, (\pm)-23a–e, and (\pm)-29a–d. This material is available free of charge via the Internet at <http://pubs.acs.org>.

■ AUTHOR INFORMATION

Corresponding Author

*Phone: +33 149424687. Fax: +33 149424658. E-mail: pierre.deprez@glpg.com.

Present Addresses

[†]Cistim, Minderbroedersstraat 12 Gebouw N, 3000 Leuven, Belgium.

[‡]Institut de Recherche Servier, 125 chemin de ronde, 78290 Croissy-sur-Seine, France.

Notes

The authors declare no competing financial interest.

■ ACKNOWLEDGMENTS

The chiral chromatographic separation was efficiently performed by Serge Droux and his team (Kyrailia SAS, Parc Biocitech, Romainville, France). We thank Kara Bortone for her careful review of the manuscript and her advice.

■ ABBREVIATIONS USED

SARM, selective androgen receptor modulator; AR, androgen receptor; ORX, orchidectomized; T, testosterone; TP, testosterone propionate; DHT, α -dihydrotestosterone; SAR, structure–activity relationship; PK, pharmacokinetic; TBS, *tert*-butyldimethylsilyl; HPLC, high-pressure liquid chromatography; AR LBD, ligand binding domain of the androgen receptor; ARE, androgen responsive element; LA, levator ani muscle; VP, ventral prostate

■ REFERENCES

(1) (a) Nieschlag, E. Testosterone Treatment Comes of Age: New Options for Hypogonadal Men. *Clin. Endocrinol. (Oxford, U. K.)* **2006**, *65*, 275–281. (b) Brueggemier, R. W.; Miller, D. D.; Witiak, D. T. In *Principles of Medicinal Chemistry*, 4th ed.; Foye, W. O., Lemke, T. L., Williams, D. A., Eds.; Williams and Wilkins: Baltimore, MD, 1995; Chapter 23, pp 486–493. (c) Basaria, S.; Dobs, A. S. Risks versus Benefits of Testosterone Therapy in Elderly Men. *Drugs Aging* **1999**, *15*, 131–142. (d) Rhoden, E. L.; Morgentaler, A. Risks of Testosterone-Replacement Therapy and Recommendations for Monitoring. *N. Eng. J. Med.* **2004**, *350*, 482–492. (e) Morgentaler, A. Testosterone and Prostate Cancer: An Historical Perspective on a Modern Myth. *Eur. Urol.* **2006**, *50*, 935–939. (f) Kicman, A. T. Pharmacology of Anabolic Steroids. *Br. J. Pharmacol.* **2008**, *154*, 502–521.

(2) (a) Narayanan, R.; Mohler, M. L.; Bohl, C. E.; Miller, D. D.; Dalton, J. T. Selective Androgen Receptor Modulators in Preclinical and Clinical Development. *Nucl. Recept. Signaling* **2008**, *6* (1), e010. (b) Jones, J. O. Improving Selective Androgen Receptor Modulator Discovery and Preclinical Evaluation. *Expert Opin. Drug Discovery* **2009**, *4* (9), 981–993.

(3) (a) Marhefka, C. A.; Gao, W.; Chung, K.; Kim, J.; He, Y.; Yin, D.; Bohl, C.; Dalton, J. T.; Miller, D. D. Design, Synthesis, and Biological Characterization of Metabolically Stable Selective Androgen Receptor Modulators. *J. Med. Chem.* **2004**, *47* (4), 993–998. (b) Kim, J.; Wu, D.; Hwang, D. J.; Miller, D. D.; Dalton, J. T. The *para* Substituent of S-3-(Phenoxy)-2-hydroxy-2-methyl-N-(4-nitro-3-trifluoromethyl-phenyl)-propionamides Is a Major Structural Determinant of in Vivo Disposition and Activity of Selective Androgen Receptor Modulators. *J. Pharmacol. Exp. Ther.* **2005**, *315* (1), 230–239.

(4) Ostowski, J.; Kuhns, J. E.; Lupisella, J. A.; Manfredi, M. C.; Beehler, B. C.; Krystek, S. R.; Jr, Bi, Y.; Sun, C.; Seethala, R.; Golla, R.; Slep, P. G.; Fura, A.; An, Y.; Kish, K. F.; Sack, J. S.; Mookhtiar, K. A.; Grover, G. J.; Hamann, L. G. Pharmacological and X-ray Structural Characterization of a Novel Selective Androgen Receptor Modulator: Potent Hyperanabolic Stimulation of Skeletal Muscle with Hypostimulation of Prostate in Rats. *Endocrinology* **2007**, *148* (1), 4–12.

(5) Long, Y. O.; Higushi, R. I.; Caferro, T. R.; Lau, T. L. S.; Wu, M.; Cummings, M. L.; Martinborough, E. A.; Marshke, K. B.; Chang, W. Y.; Lopez, F. J.; Karanewsky, D. S.; Zhi, L. Selective Androgen Receptor Modulators Based on a Series of 7H-[1,4]Oxazino[3,2-g]quinolin-7-ones with Improved in Vivo Activity. *Bioorg. Med. Chem. Lett.* **2008**, *18* (9), 2967–2971.

(6) Nique, F.; Hebbe, S.; Peixoto, C.; Annoot, D.; Lefrançois, J.-M.; Duval, E.; Michoux, L.; Triballeau, N.; Lemoullac, J.-M.; Mollat, P.; Thauvin, M.; Prangé, T.; Minet, D.; Clément-Lacroix, P.; Robin-Jagerschmidt, C.; Fleury, D.; Guédin, D.; Deprez, P. Discovery of Diarylhydantoin as New Selective Androgen Receptor Modulators (SARMs). *J. Med. Chem.* **2012**, DOI: 10.1021/jm300249m.

(7) Mandagere, A. K.; Thompson, T. N.; Hwang, K. Graphical Model for Estimating Oral Bioavailability of Drugs in Humans and Other Species from Their Caco-2 Permeability and in Vitro Liver Enzyme Metabolic Stability Rates. *J. Med. Chem.* **2002**, *45*, 304–311.

(8) *N*-Tosylindole-5-methyl ketone **5a** and *N*-((2-(trimethylsilyl)ethoxy)methyl)benzimidazole-5-methyl ketone **5b** were prepared in three or four steps from indole-5-carboxaldehyde or methyl *1H*-benzimidazole-5-carboxylate, and the syntheses are reported in the Supporting Information.

(9) The synthesis of compounds **10a–i** and **11a,b** is described in the Supporting Information. 1-Aryl-2-hydroxyethanones were directly protected with allyl bromide to give **10a–c** (in 33–63% yield).¹⁰ In a two-step sequence, 1-aryl-2-bromoethanones provided **10d–h** (in 23–53% yield over two steps). Finally, 2-(allyloxy)-1-*m*-tolylethanone (**10i**) was synthesized in three steps starting from 3'-methylacetophenone (in 25% yield over three steps).¹¹ 1-Heteroaryl-2-(benzyloxy)ethanones **11a,b** were prepared in moderate yield (23–36%) from (benzyloxy)acetyl chloride and heteroarylboronic acid by a palladium-catalyzed coupling reaction.¹²

(10) Molander, G. A.; McKie, J. A. Stereochemical Investigations of Samarium(II) Iodide-Promoted 5-Exo and 6-Exo Ketyl–Olefin Radical Cyclization Reactions. *J. Org. Chem.* **1995**, *60*, 872–882.

(11) (a) Shue, H.-J.; Chen, X.; Schwerdt, J. H.; Paliwal, S.; Blythin, D. J.; Lin, L.; Gu, D.; Wang, C.; Reichard, G. A.; Wang, H.; Piwinski, J. J.; Duffy, R. A.; Lachowicz, J. E.; Coffin, V. L.; Nomeir, A. A.; Morgan, C. A.; Varty, G. B.; Shih, N.-Y. Cyclic Urea Derivatives as Potent NK₁ Selective Antagonists. Part II: Effects of Fluoro and Benzylic Methyl Substitutions. *Bioorg. Med. Chem. Lett.* **2006**, *16*, 1065–1069. (b) Utsukihara, T.; Nakamura, H.; Watanabe, M.; Akira Horiuchi, C. Microwave-Assisted Synthesis of α -Hydroxy Ketone and α -Diketone and Pyrazine Derivatives from α -Halo and α,α' -Dibromo Ketone. *Tetrahedron Lett.* **2006**, *47*, 9359–9364.

(12) Fujii, N.; Mallari, J. P.; Hansell, E. J.; Mackey, Z.; Doyle, P.; Zhou, Y. M.; Gut, J.; Rosenthal, P. J.; McKerrow, J. H.; Kiplin Guy, R. Discovery of Potent Thiosemicarbazone Inhibitors of Rhodensin and Cruzain. *Bioorg. Med. Chem. Lett.* **2005**, *15*, 121–123.

(13) Commercially available from Apollo Scientific (CAS 6321-86-4) or synthesis reported in the literature in three steps from 2-oxophenylethyl acetate: Henze, H.; Winfred, C. The Interaction of Certain α -(4-Morpholinyl)alkyl Aryl Ketones with Potassium Cyanide and Ammonium Carbonate. *J. Org. Chem.* **1945**, *10*, 2–9.

(14) The synthesis of compound **25** is described in the Supporting Information.

(15) HPLC: Chiralcel OD, column 250 × 4.6 mm, heptane/2-propanol (75/25), flow rate 1 mL/min.

(16) Olma, A. α -Hydroxymethylphenylglycine and α -Hydroxymethylphenylalanine: Synthesis, Resolution and Absolute Configuration. *Pol. J. Chem.* **1996**, *70*, 1442–1447.

(17) Garcia, H. G.; Kondev, J.; Orme, N.; Theriot, J. A.; Phillips, R. Thermodynamics of Biological Processes. *Methods Enzymol.* **2011**, *492*, 27–59.

(18) Thauvin, M.; Robin-Jagerschmidt, C.; Nique, F.; Mollat, P.; Fleury, D.; Prangé, T. Crystallization and Preliminary X-ray Analysis of the Human Androgen Receptor Ligand-Binding Domain with a Coactivator-like Peptide and Selective Androgen Receptor Modulators. *Acta Crystallogr.* **2008**, *F64*, 1159–1162.

(19) Bohl, C. E.; Miller, D. D.; Chen, J.; Bell, C. E.; Dalton, J. T. Structural Basis for Accommodation of Nonsteroidal Ligands in the Androgen Receptor. *J. Biol. Chem.* **2005**, *280* (45), 37747–37754.

(20) Brzozowski, A. M.; Pike, A. C.; Dauter, Z.; Hubbard, R. E.; Bonn, T.; Engström, O.; Ohman, L.; Greene, G. L.; Gustafsson, J. A.; Carlquist, M. Molecular Basis of Agonism and Antagonism in the Oestrogen Receptor. *Nature* **1997**, Oct 16, 389 (6652), 753–758.

(21) (a) Eisenberg, E.; Gordan, G. S. The Levator Ani of the Rat as an Index of Myotrophic Activity of Steroidal Hormones. *J. Pharmacol. Exp. Ther.* **1950**, *99* (1), 38–44. (b) Hershberger, L. G.; Shipley, E. G.; Meyer, R. K. Myotrophic Activity of 19-Nortestosterone and Other Steroids Determined by Modified Levator Ani Muscle Method. *Proc. Soc. Exp. Biol. Med.* **1953**, *83* (1), 175–180. (c) Kicman, A. T. Pharmacology of Anabolic Steroids. *Br. J. Pharmacol.* **2008**, *154* (3), 502–521.

(22) Momany, F. A.; Rone, R. J. Validation of the General Purpose QUANTA 3.2/CHARMm Force Field. *J. Comput. Chem.* **1992**, *13*, 888–900.

(23) Venkatachalam, C. M.; Jiang, X.; Oldfield, T.; Waldman, M. LigandFit: A Novel Method for the Shape-Directed Rapid Docking of Ligands to Protein Active Sites. *J. Mol. Graphics Modell.* **2003**, *21*, 289–307.

(24) Mayo, S. L.; Olafson, B. D.; Goddard, W. A. DREIDING: A Generic Force Field for Molecular Simulations. *J. Phys. Chem.* **1990**, *94*, 8897–8909.

(25) Krammer, A.; Kirchhoff, P. D.; Jiang, X.; Venkatachalam, C. M.; Waldman, M. LigScore: A Novel Scoring Function for Predicting Binding Affinities. *J. Mol. Graphics Modell.* **2005**, *23*, 395–407.